*Inorg. Chem.* **2006**, *45*, 1012–1020


# Malonate-Containing Manganese(III) Complexes: Synthesis, Crystal Structure, and Magnetic Properties of $AsPh_4[Mn(mal)_2(H_2O)_2]$

**Fernando S. Delgado,[†] Nicolas Kerbellec,[‡] Catalina Ruiz-Pérez,*[,†] Joan Cano,[§] Francesc Lloret,[‡] and Miguel Julve[‡]**

*Laboratorio de Rayos X y Materiales Moleculares, Departamento de Física Fundamental II, Facultad de Física, Universidad de La Laguna, Avda, Astrofísico Francisco Sánchez s/n, 38204 La Laguna, Tenerife, Spain, Departament de Química Inorgànica/Instituto de Ciencia Molecular, Facultat de Química de la Universitat de València, Dr. Moliner 50, 46100-Burjassot, València, Spain, and Institució Catalana de Recerca i Estudis Avançats (ICREA)/Departament de Química Inorgànica i Centre de Recerca en Química Teórica, Universitat de Barcelona, Diagonal 647, 08028 Barcelona, Spain*

Received May 26, 2005

The novel manganese(III) complexes $PPh_4[Mn(mal)_2(H_2O)_2]$ (**1**) and $AsPh_4[Mn(mal)_2(H_2O)_2]$ (**2**) ($PPh_4^+$ = tetraphenylphosphonium cation, $AsPh_4^+$ = tetraphenylarsonium cation, and $H_2mal$ = malonic acid) have been prepared, and the structure of **2** was determined by X-ray diffraction analysis. **2** is a mononuclear complex whose structure is made up of *trans*-diaquabis(malonato)manganate(III) units and tetraphenylarsonium cations. Two crystallographically independent manganese(III) ions (Mn(1) and Mn(2)) occur in **2** that exhibit elongated octahedral surroundings with four oxygen atoms from two bidentate malonate groups in equatorial positions (Mn(1)–O = 1.923(6) and 1.9328(6) Å and Mn(2)–O = 1.894(6) and 1.925(6) Å) and two trans-coordinated water molecules in the axial sites (Mn(1)–Ow = 2.245(6) Å and Mn(2)–Ow = 2.268(6) Å). The $[Mn(mal)_2(H_2O)_2]^-$ units are linked through hydrogen bonds involving the free malonate–oxygen atoms and the coordinated water molecules to yield a quasi-square-type anionic layer growing in the *ab* plane. The shortest intralayer metal–metal separations are 7.1557(7) and 7.1526(7) Å (through the edges of the square). The anionic sheets are separated from each other by layers of $AsPh_4^+$ where sextuple- and double-phenyl embraces occur. The magnetic behavior of **1** and **2** in the temperature range 1.9–290 K reveals the occurrence of weak intralayer ferromagnetic interactions ($J$ = +0.081(1) (**1**) and +0.072(2) $cm^{-1}$ (**2**)). These values are compared to those of the weak antiferromagnetic coupling [$J$ = –0.19(1) $cm^{-1}$], which is observed in the chain compound $K_2[Mn(mal)_2(MeOH)_2][Mn(mal)_2]$ (**3**), where the exchange pathway involves the carboxyate–malonate bridge in the anti–syn conformation. The structure of **3** was reported elsewhere. Theoretical calculations on fragment models of **2** and **3** were performed to analyze and substantiate both the nature and magnitude of the magnetic couplings observed.

## Introduction

The use of deprotonated dicarboxylic acids as bridging ligands between paramagnetic transition-metal ions to afford polynuclear compounds is an area of continuous interest both in molecular magnetism[1] and in biology.[2] Among the first-row transition-metal ions, the case of carboxylato-bridged manganese(II) complexes is specially relevant because such systems are known to exist at the active centers of some manganese-containing enzymes.[3] Focusing on the magnetic studies and without being exhaustive, examples are known of structurally characterized oxalate-,[4] terephthalate-,[5] adipate-,[6] and malonate-bridged[7] manganese(II) compounds with antiferromagnetic interactions ranging from maximum values of −2.5 (through oxalato) to −0.70 $cm^{-1}$ (through carboxy-

* To whom correspondence should be addressed. E-mail: caruiz@ull.es.
† Universidad de La Laguna.
‡ Universitat de València.
§ Universitat de Barcelona.

(1) (a) Oldham, C. In *Comprehensive Coordination Chemistry*; Wilkinson, G., Gillard, R. D., McCleverty, J. A., Eds.; Pergamon Press: Oxford, U.K., 1987; Vol. 2, p 435. (b) Kahn, O. *Molecular Magnetism*; VCH: New York, 1993.

(2) Christou, G. *Acc. Chem. Res.* **1989**, *22*, 328. (b) Wieghardt, K. *Angew. Chem., Int. Ed. Engl.* **1989**, *28*, 1153.



10.1021/ic0508526 CCC: $33.50 
Published on Web 01/11/2006

late−malonate). The case of the malonate dianion (hereafter noted as mal) is very appealing mainly due to two features which are well illustrated by its copper(II) complexes: (i) the great versatility as a ligand given that it can adopt not only the chelating bidentate coordination mode but also the *syn*−*syn*, *syn*−*anti*, and *anti*−*anti* carboxylate-bridging modes; (ii) the ability to mediate ferromagnetic interactions between the metal ions that it bridges.[8−11] Interestingly, this ferromagnetic interaction between the copper(II) ions through the carboxylate−malonate bridge is kept when one of the hydrogen atoms of the methylene group is replaced by a phenyl group (that is, phenylmalonate as the ligand instead of malonate).[12]

The extensive magneto−structural work that has been carried out with the malonate complexes with divalent first-row transition-metal ions[7−11,13] contrasts with the paucity of investigations concerning the manganese(III) ion.[14−16] The coordination chemistry of this cation is not an easy task because of its fairly oxidizing power and easy disproportion. However, its presence in discrete polynuclear transition-metal complexes, which exhibit a slow relaxation of the magnetization,[17] have caught the eyes of magnetochemists interested in the design of molecular magnets. This property is strongly related to the occurrence of a large spin in the ground state and a strong axial anisotropy in the cluster. This last requirement can be fulfilled by the presence of Mn(III), known to possess a pronounced magnetic anisotropy. In the search for stable manganese(III) building blocks to be used as precursors of these so-called single-molecule magnets, we have prepared the new manganese(III) complexes $PPh_4[Mn(mal)_2(H_2O)_2]$ (**1**) and $AsPh_4[Mn(mal)_2(H_2O)_2]$ (**2**) ($PPh_4^+$ = tetraphenylphosphonium cation, $AsPh_4^+$ = tetraphenylarsonium cation, and $H_2mal$ = malonic acid). Their preparation, structural characterization, magnetic study, and a theoretical analysis of the exchange pathway are presented here. The magnetic properties of the previously reported chain compound $K_2[Mn(mal)_2(MeOH)_2][Mn(mal)_2]$[14b] (**3**) were investigated for comparison.

## Experimental Section

**Materials.** Malonic acid, potassium permanganate, tetraphenylphosphonium chloride, and tetraphenylarsonium chloride monohydrate were purchased from commercial sources and used as received. Polycrystalline samples of $K_2[Mn(mal)_2(MeOH)_2][Mn(mal)_2]$ (**3**) were prepared by the method of Cartledge and Nichols,[18] and well-formed green crystals of this compound were grown by the receipt of Lis and Matuszewski.[14a] These crystals, once crushed, were used for the magnetic measurements. Elemental analyses (C, H) were carried out by the Microanalytical Service of the Universidad Autónoma de Madrid. The X−Mn (X = P (**1**), As (**2**), and K (**3**)) molar ratio was determined by electron probe X-ray microanalysis at the Servicio Interdepartamental de Investigación de la Universidad de Valencia.

**Preparation of $PPh_4[Mn(mal)_2(H_2O)_2]$ (1) and $AsPh_4[Mn(mal)_2(H_2O)_2]$ (2).** **1** and **2** were obtained as polycrystalline, olive-green powders by adding solid $PPh_4Cl$ (1 mmol, **1**) and $AsPh_4Cl\cdot H_2O$ (1 mmol, **2**) to an aqueous solution (30 mL, 0.05 M $H_2mal$) of $K_2[Mn(mal)_2(MeOH)_2][Mn(mal)_2]$ (1 mmol, **1** and **2**). The yield


(3) (a) *Manganese Redox Enzymes*; Pecoraro, V. L., Ed.; VCH: New York, 1992. (b) Waldo, G. S.; Yu, S.; Penner-Hahn, J. E. *J. Am. Chem. Soc.* **1992**, *114*, 5869. (c) Tan, X. S.; Xiang, D. F.; Tang, W. X.; Sun, J. *Polyhedron* **1997**, *16*, 689. (d) Policar, C.; Lambert, F.; Cesario, M.; Morgenstern-Badarau, I. *Eur. J. Inorg. Chem.* **1999**, 2201. (e) Tangoulis, V.; Psomas, G.; Dendrinou-Samara, C.; Raptopoulou, C. P.; Terzis, A.; Kessissoglou, D. P. *Inorg. Chem.* **1996**, *35*, 7655. (f) Albela, B.; Corbella, M.; Ribas, J.; Castro, I.; Sletten, J.; Stoeckli-Evans, H. *Inorg. Chem.* **1998**, *37*, 788. (g) Xen, X. M.; Tong, Y. X.; Xu, Z. T.; Mak, T. C. W. *J. Chem. Soc., Dalton Trans.* **1995**, 4001.

(4) (a) Verdaguer, M. Ph.D. Thesis, University of Orsay, France, 1984. (b) Deguenon, D.; Bernardelli, G.; Tuchagues, J. P.; Castan, P. *Inorg. Chem.* **1990**, *29*, 3031. (c) Ménage, S.; Vítols, S. E.; Bergerat, P.; Codjovi, E.; Kahn, O.; Girerd, J. J.; Guillot, M.; Solans, X.; Calvet, T. *Inorg. Chem.* **1991**, *30*, 2666. (d) Glerup, J.; Goodson, P. A.; Hodgson, D. J.; Michelsen, K. *Inorg. Chem.* **1995**, *34*, 6255. (e) Marinescu, G.; Andruh, M.; Lescouëzec, R.; Muñoz, M. C.; Cano, J.; Lloret, F. *New J. Chem.* **2000**, *24*, 527.

(5) Cano, J.; De Munno, G.; Sanz, J.; Ruiz, R.; Lloret, F.; Faus, J.; Julve, M. *J. Chem. Soc., Dalton Trans.* **1994**, 3465.

(6) Kim, Y. J.; Jung, D. Y. *Inorg. Chem.* **2000**, *39*, 1470.

(7) (a) Lis, T.; Matuszewski, *Acta Crystallogr., Sect. B: Struct. Sci.* **1979**, *35*, 2212. (b) Sain, S.; Maji, T. K.; Mostafa, G.; Lu, T. H.; Chaudhuri, N. R. *Inorg. Chim. Acta* **2003**, *351*, 12. (c) Rodríguez-Martín, Y.; Hernández-Molina, M.; Sanchiz, J.; Ruiz-Pérez, C.; Lloret, F.; Julve, M. *Dalton Trans.* **2003**, 2359. (d) Maji, T. K.; Sain, S.; Mostafa, G.; Lu, T. H.; Ribas, J.; Monfort, M.; Chaudhuri, N. R. *Inorg. Chem.* **2003**, *42*, 709.

(8) Sain, S.; Maji, T. K.; Mostafa, G.; Lu, T. H.; Chaudhuri, N. R. *New J. Chem.* **2003**, *27*, 185.

(9) Liu, T. F.; Sun H. L.; Gao, S.; Zhang, S. W.; Lau, T. C. *Inorg. Chem.* **2003**, *42*, 4792.

(10) Zhang, X.; Lu, C.; Zhang, Q.; Lu, S.; Yang, W.; Liu, J.; Zhuang, H. *Eur. J. Inorg. Chem.* **2003**, 1181.

(11) (a) Ruiz-Pérez, C.; Sanchiz, J.; Hernández-Molina, M.; Lloret, F.; Julve, M. *Inorg. Chem.* **2000**, *39*, 1363 (b) Ruiz-Pérez, C.; Hernández-Molina, M.; Lorenzo-Luis, P.; Lloret, F.; Cano, J.; Juve, M. *Inorg. Chem.* **2000**, *39*, 3845. (c) Sanchiz, J.; Rodríguez-Martín, Y.; Ruiz-Pérez, C.; Mederos, A.; Lloret, F.; Julve, M. *New J. Chem.* **2002**, *26*, 1624. (d) Rodríguez-Martín, Y.; Ruiz-Pérez, C.; Sanchiz, J.; Lloret, F.; Julve, M. *Inorg. Chim. Acta* **2001**, *318*, 159. (e) Rodríguez-Martín, Y.; Hernández-Molina, M.; Delgado, F. S.; Pasán, J.; Ruiz-Pérez, C.; Sanchiz, J.; Lloret, F.; Julve, M. *CrystEngComm* **2002**, *4*, 440. (f) Rodríguez-Martín, Y.; Hernández-Molina, M.; Delgado, F. S.; Pasán, J.; Ruiz-Pérez, C.; Sanchiz, J.; Lloret, F.; Julve, M. *CrystEngComm* **2002**, *4*, 522. (g) Delgado, F. S.; Sanchiz, J.; Ruiz-Pérez, C.; Lloret, F.; Julve, M. *Inorg. Chem.* **2003**, *42*, 5938. (h) Ruiz-Pérez, C.; Rodríguez-Martín, Y.; Hernández-Molina, M.; Delgado, F. S.; Pasán, J.; Sanchiz, J.; Lloret, F.; Julve, M. *Polyhedron* **2003**, *22*, 2111. (i) Pasán, J.; Delgado, F. S.; Rodríguez-Martín, Y.; Hernández-Molina, M.; Ruiz-Pérez, C.; Sanchiz, J.; Lloret, F.; Julve, M. *Polyhedron* **2003**, *22*, 2143.

(12) (a) Pasán, J.; Sanchiz, J.; Ruiz-Pérez, C.; Lloret, F.; Julve, M. *New J. Chem.* **2003**, *27*, 1557. (b) Pasán, J.; Sanchiz, J.; Ruiz-Pérez, C.; Lloret, F.; Julve, M. *Eur. J. Inorg. Chem.* **2004**, 4081.

(13) (a) Chattopadhyay, D.; Chatttopadhyay, S. K.; Lowe, P. R.; Schwalbe, C.; Gil de Muro, I.; Mautner, F. A.; Insausti, M.; Lezama, L.; Arriortua, M. I.; Rojo, T. *Inorg. Chem.* **1998**, *37*, 3243. (b) Ruiz-Pérez, C.; Sanchiz, J.; Hernández-Molina, M.; Lloret, F.; Julve, M. *Inorg. Chim. Acta* **2000**, *298*, 202. (c) Ruiz-Pérez, C.; Hernández-Molina, M.; Sanchiz, J.; López, T.; Lloret, F.; Julve, M. *Inorg. Chim. Acta* **2000**, *298*, 245. (d) Rodríguez-Martín, Y.; Sanchiz, J.; Ruiz-Pérez, C.; Lloret, F.; Julve, M. *CrystEngComm* **2002**, *4*, 631. (e) Delgado, F. S.; Sanchiz, J.; Ruiz-Pérez, C.; Lloret, F.; Julve, M. *CrystEngComm* **2003**, *5*, 280. (f) Delgado, F. S.; Hernández-Molina, M.; Sanchiz, J.; Ruiz-Pérez, C.; Rodríguez-Martín, Y.; López, T.; Lloret, F.; Julve, M. *CrystEngComm* **2004**, *6*, 106.

(14) (a) Lis, T.; Matuszewski, J. *J. Chem. Soc., Dalton Trans.* **1980**, 996. (b) Kirk, M. L.; Lah, M. S.; Raptopoulou, C.; Kessissoglou, D. P.; Hatfield, W. E.; Pecoraro, V. L. *Inorg. Chem.* **1991**, *30*, 3900.

(15) Wei, Y. G.; Zhang, S. W.; Shao, M. C.; Shao, M. C.; Liu, Q.; Tang, Y. Q. *Polyhedron* **1996**, *15*, 4303.

(16) (a) Lis, T.; Matuszewski, J.; Jezowska-Trzebiatowska, B. *Acta Crystallogr.* **1977**, *B33*, 1943. (b) Lis, T.; Matuszewski, *Polish J. Chem.* **1980**, *54*, 163.

(17) (a) (a) Barra, A. L.; Gatteschi, D.; Sessoli, R. *Phys. Rev.* **1997**, *B56*, 8192. (b) Yoo, J.; Yamaguchi, A.; Nakano, M.; Krzystek, J.; Streib, W. E.; Brunel, L. C.; Ishimoto, H.; Christou, G.; Hendrickson, D. N. *Inorg. Chem.* **2001**, *40*, 4604. (c) Gatteschi, D. Sessoli, R. *Angew. Chem., Int. Ed.* **2003**, *42*, 269.

(18) Cartledge, G. H.; Nichols, P. M. *J. Am. Chem. Soc.* **1940**, *62*, 3057.

was ~70%. The recrystallization of these powder samples in a 1:2 $H_2O-MeOH$ (v/v) mixture in a hood afforded platelike crystals of **1** and rods of **2**. The rods were suitable for X-ray diffraction, whereas the plates poorly diffract. Anal. Calcd for $C_{30}H_{28}MnO_{10}P$ (**1**): C, 56.81; H, 4.42. Found: C, 56.45; H, 4.36. Anal. Calcd for $C_{30}H_{28}AsMnO_{10}$ (**2**): C, 53.13; H, 4.12. Found: C, 52.93; H, 4.06. Selected IR peaks (KBr disk, $cm^{-1}$): 3500−3200 s,br (**1** and **2**) [$\nu$(O−H)], 2904 w (**1**) and 2908 w (**2**) [$\nu$(C−H)], 1636 s,sh (**1** and **2**) [$\nu_a(COO^-)$], 1368 s,sh (**1**) and 1363 s,sh (**2**) [$\nu_s(COO^-)$], 789, 759, 722, and 691 m,sh (**1**) and 795, 750, and 690 m,sh (**2**) [$\delta$(C−H)].

**Physical Techniques.** IR spectra (4000−400 $cm^{-1}$) were recorded on a Bruker IF S55 spectrophotometer with samples prepared as KBr pellets. Variable-temperature (1.9−295 K) magnetic-susceptibility measurements on polycrystalline samples of **1**−**3** were carried out with a Quantum Design SQUID operating at 5000 Oe in the high-temperature range (30−295 K) and at 250 Oe at $T <$ 30 K to avoid saturation phenomena. Diamagnetic corrections for the molar units were estimated from Pascal constants[19] as $-365 \times 10^{-6}$ (**1**), $-370 \times 10^{-6}$ (**2**), and $-141 \times 10^{-6}$ $cm^3$ $mol^{-1}$ (**3**) (per mol of manganese(III)).

**Computational Strategy.** All theoretical calculations were carried out with the hybrid B3LYP method,[20−22] as is implemented in Gaussian03 program.[23] Double- and triple-$\zeta$ quality basis sets proposed by Ahlrichs and co-workers have been used for all atoms.[24,25] The broken-symmetry approach has been employed to describe the unrestricted solutions of the antiferromagnetic spin states.[26−29] Two models have been built from the experimental crystal structure to analyze the magnetic interactions between the manganese(III) ions in **2** and **3** (see Figure 9). A quadratic convergence method was used to determine the more-stable wave functions in the SCF process.[30] The atomic spin densities were obtained from natural bond orbital (NBO) analysis.[31−33]

**Table 1.** Crystal Data and Details of Structure Determination

| | |
|---|---|
| cpmpd | **2** |
| formula | $C_{30}H_{24}AsMnO_{10}$ |
| $M$ | 674.35 |
| cryst syst | triclinic |
| space group | $P\bar{1}$ |
| $a$, Å | 9.8888(8) |
| $b$, Å | 10.3411(13) |
| $c$, Å | 14.136(2) |
| α, deg | 85.499(4) |
| $\beta$, deg | 84.737(6) |
| $\gamma$, deg | 89.975(7) |
| $V$, Å$^3$ | 1435.0(3) |
| $Z$ | 2 |
| $T$, K | 293(2) |
| $\rho_{calc}$, Mg $m^{-3}$ | 1.561 |
| $\lambda$, Mo−Kα, Å | 0.71073 |
| $\mu$, Mo−Kα, $mm^{-1}$ | 1.662 |
| R1, $I > 2\sigma(I)$ (all) | 0.090 (0.150) |
| wR2, $I > 2\sigma(I)$ (all) | 0.205 (0.255) |
| measured reflns ($R_{int}$) | 11083 (0.074) |
| independent reflns [$I > 2\sigma$(I)] | 5426 (3526) |

**Crystal Data Collection and Refinement.** A single crystal of **2** was mounted on a Bruker-Nonius KappaCCD diffractometer. Orientation matrix and lattice parameters were obtained by least-squares refinement of the reflections obtained by a $\theta-\chi$ scan (Dirax/lsq method). Diffraction data of **2** were collected at 293(2) K using graphite-monochromated Mo $K_\alpha$ radiation ($\lambda$ = 0.71073 Å). A summary of the crystallographic data and structure refinement is given in Table 1. The indexes of data collection were $-11 \le h \le 11$, $-12 \le k \le 12$, and $-11 \le l \le 17$. Of the 5426 measured independent reflections in the $\theta$ range 1.98−26° (**2**), 3526 have $I \ge 2\sigma(I)$. The sample diffracts weakly over 26°. All of the measured independent reflections were used in the analysis. All calculations for data reduction, structure solution, and refinement were done by standard procedures (WINGX).[34] The structure was solved by direct methods and refined with the full-matrix least-squares technique on $F^2$ using the SHELXS-97[35] and SHELXL-97[35] programs. The hydrogen atoms of the malonate and tetraphenylarsonium groups were set in calculated positions and isotropically refined as riding atoms. The hydrogen atoms of the water molecules were not found. The final Fourier-difference map showed maximum- and minimum-height peaks of 0.843 and −0.806 e $Å^{-3}$, respectively. The final geometrical calculations and the graphical manipulations were carried out with PARST97,[36] CRYSTAL MAKER,[37] and DIAMOND[38] programs. Selected bond distances and angles for **2** are listed in Table 2. The CCDC reference number for **2** is 271896.

## Results and Discussion

**Description of the Structure of 2.** The solid-state structure of **2** comprises *trans*-diaquabis(malonato)manganate(III) anions and tetraphenylarsonium cations, which are linked through electrostatic forces, hydrogen bonds, and van der Waals interactions. Two crystallographically independent


(19) Earnshaw, A. *Introduction to Magnetochemistry*, Academic Press: London and New York, 1968.
(20) Becke, A. D. *Phys. Rev. A* **1988**, *38*, 3098.
(21) Lee, C.; Yang, W.; Parr, R. G. *Phys. Rev. B* **1988**, *37*, 785.
(22) Becke, A. D. *J. Chem. Phys.* **1993**, *98*, 5648.
(23) Frisch, M. J.; Trucks, G. W.; Schlegel, H. B.; Scuseria, G. E.; Robb, M. A.; Cheeseman, J. R.; Montgomery, J. A.; Vreven, Jr., T.; Kudin, K. N.; Burant, J. C.; Millam, J. M.; Iyengar, S. S.; Tomasi, J.; Barone, V.; Mennucci, B.; Cossi, M.; Scalmani, G.; Rega, N.; Petersson, G. A.; Nakatsuji, H.; Hada, M.; Ehara, M.; Toyota, K.; Fukuda, R.; Hasegawa, J.; Ishida, M.; Nakajima, T.; Honda, Y.; Kitao, O.; Nakai, H.; Klene, M.; Li, X.; Knox, J. E.; Hratchian, H. P.; Cross, J. B.; Bakken, V.; Adamo, C.; Jaramillo, J.; Gomperts, R.; Stratmann, R. E.; Yazyev, O.; Austin, A. J.; Cammi, R.; Pomelli, C.; Ochterski, J. W.; Ayala, P. Y.; Morokuma, K.; Voth, G. A.; Salvador, P.; Dannenberg, J. J.; Zakrzewski, V. G.; Dapprich, S.; Daniels, A. D.; Strain, M. C.; Farkas, O.; Malick, D. K.; Rabuck, A. D.; Raghavachari, K.; Foresman, J. B.; Ortiz, J. V.; Cui, Q.; Baboul, A. G.; Clifford, S.; Cioslowski, J.; Stefanov, B. B.; Liu, G.; Liashenko, A.; Piskorz, P.; Komaromi, I.; Martin, R. L.; Fox, D. J.; Keith, T.; Al-Laham, M. A.; Peng, C. Y.; Nanayakkara, A.; Challacombe, M.; Gill, P. M. W.; Johnson, B.; Chen, W.; Wong, M. W.; González, C.; Pople, J. A. *Gaussian 03*, Revision C.02.; Gaussian, Inc.: Wallingford, CT, 2004.
(24) Schaefer, A.; Horn, A.; Ahlrichs, R. *J. Chem. Phys.* **1992**, *97*, 2571.
(25) Schaefer, A.; Huber, C.; Ahlrichs, R. *J. Chem. Phys.* **1994**, *100*, 5829.
(26) Cano, J.; Alemany, P.; Alvarez, S.; Verdaguer, M.; Ruiz, E. *Chem. Eur. J.* **1998**, *4*, 476.
(27) Ruiz, E.; Cano, J.; Alvarez, S.; Alemany, P. *J. Am. Chem. Soc.* **1998**, *120*, 11122.
(28) Ruiz, E.; Cano, J.; Alvarez, S.; Alemany, P. *J. Comput. Chem.* **1999**, *20*, 1391.
(29) Cano, J.; Ruiz, E.; Alemany, P.; Lloret, F.; Alvarez, S. *J. Chem. Soc., Dalton Trans.* **1999**, 1669.
(30) Bacskay, G. B. *Chem. Phys.* **1981**, *61*, 385.
(31) Carpenter, J. E.; Weinhold, F.; *J. Mol. Struct. (THEOCHEM)* **1988**, *169*, 41.
(32) Reed, A. E.; Curtis, L. A.; Weinhold, F. *Chem. Rev.* **1988**, *88*, 899.
(33) Weinhold, F.; Carpenter, J. E. *The Structure of Small Molecules and Ions*; Plenum: New York, 1988; p 227.
(34) Farrugia, L. J. WINGX, *J. Appl. Cryst*, **1999**, *32*, 837.
(35) Sheldrick, G. M. *SHELX97*, Programs for Crystal Structure Anlysis (Release 97-2), Institüt für Anorganische Chemie der Universität: Göttingen, Germany, 1998.
(36) Nardelli, M. *J. Appl. Crystallogr.* **1995**, *28*, 659.
(37) *CRYSTAL MAKER* 4.2.1. Crystalmaker Sofware: Oxfordside, UK, 2001.
(38) *DIAMOND 2.1d, Crystal Impact GbR, CRYSTAL IMPACT, K*; Brandenburg & H. Putz GbR: Bonn, Germany, 2000.

**Table 2.** Selected Bond Lengths (Å) and Angles (deg) for **2**

| | | | |
|---|---|---|---|
| Mn(1)−O(1) | 1.923(6) | Mn(2)−O(11) | 1.894(6) |
| Mn(1)−O(2) | 1.932(6) | Mn(2)−O(12) | 1.925(6) |
| Mn(1)−O(1w) | 2.245(6) | Mn(2)−O(2w) | 2.268(6) |
| O(1)−Mn(1)-O(2) | 91.7(3) | O(11)−Mn(2)-O(12) | 91.5(3) |
| O(1)−Mn(1)-O(2a)[a] | 88.3(3) | O(11)−Mn(2)-O(12b)[a] | 88.5(3) |
| O(1)−Mn(1)-O(1w) | 90.9(2) | O(11)−Mn(2)-O(2w) | 89.5(2) |
| O(1)−Mn(1)-O(1wa)[a] | 89.1(2) | O(11)−Mn(2)-O(2wb)[a] | 90.5(2) |
| O(2)−Mn(1)-O(1w) | 93.1(2) | O(12)−Mn(2)-O(2w) | 88.7(2) |
| O(2)−Mn(1)-O(1wa)[a] | 86.9(2) | O(12)−Mn(2)-O(2wb)[a] | 91.3(2) |

[a] Symmetry codes: (a) $-x, -y, -z$; (b) $-x + 1, -y + 1, -z$.

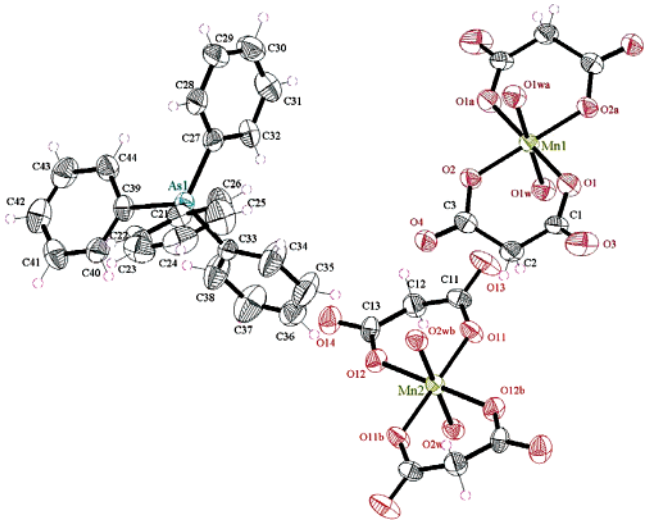


**Figure 1.** Perspective view showing the two crystallographically independent metal ions (Mn(1), Mn(2)) and the $AsPh_4^+$ cation in **2**. Thermal ellipsoids are drawn at the 50% probability level.

manganese(III) units (Mn(1) and Mn(2)) occur in **2** (see Figure 1), the manganese atoms being located on crystallographic inversion centers. The manganese atoms are six-coordinated with four coplanar oxygen atoms from two bidentate malonate ligands in the equatorial plane (the mean Mn−O(mal) bond distances being 1.928(6) and 1.910(6) Å for Mn(1) and Mn(2), respectively), whereas the axial positions are filled by two water molecules (2.245(6) and 2.268(6) Å for Mn(1)−O(1w) and Mn(2)−O(2w), respectively). The resulting $MnO_6$ elongated octahedron has geometric values $\phi = 55.88$ and $s/h = 1.341$ at Mn(1) and $\phi = 55.57$ and $s/h = 1.361$ at Mn(2), with $\phi$ and $s/h$ being the twist angle and the compression ratio, respectively.[39] The values of the average Mn−O(malonate) bonds of **2** agree with those observed in the related mononuclear compound $K[Mn(mal)_2(H_2O)_2]\cdot 2H_2O$ (1.90 Å).[16a] As far as for the values of 2.245(6) and 2.268(6) Å for the Mn−$O_w$ bond distance in **2**, they are rather long for coordinated water, indicating that this bond is quite weak. However, they compare well with the value of 2.30 Å reported for this bond in the compound $K[Mn(mal)_2(H_2O)_2]\cdot 2H_2O$.[16a] Such marked axial elongations are typical of high-spin $d^4$ systems.

Two crystallographycally independent malonate ions are present in **2**. They act as bidentate ligands toward the manganese(III) ions, the values of the angles subtended at the metal atom being 91.7(3)° (O(1)−Mn(1)−O(2)) and 91.5(3)° (O(11)−Mn(2)−O(12)). Each malonate ligand exhibits a twist-boat conformation.[40] The values of the C−C (1.488(13)−1.518(13) Å) and C−O (1.219(10)−1.289(10) Å) malonate bond distances and O−C−O (118.3(8)−121.2(9)°) bond angles agree well with those previously reported for malonic acid[41] and other malonate-containing metal complexes.[11,13,14a−16] The $[Mn^{III}(mal)_2(H_2O)_2]^-$ units are linked through hydrogen-bonds involving the free malonate−oxygen atoms and the coordinated water molecules (see Table 3), leading to a quasi square, two-dimensional anionic network in the *ab* plane (see Figure 2). The shortest manganese···manganese intralayer distances are 7.1557(7) (Mn(1)···Mn(2)), 7.1526(7) (Mn(1)···Mn(2e); (e) $x - 1, y, z$), 9.8890(8) (Mn(1)···Mn(1f); (f) $x, y + 1, z$), and 10.3410(13) Å (Mn(2)···Mn(2e)).

**Table 3.** Relevant H-bond Distances (Å) for **2**

| D···A | |
|---|---|
| O(1w)···O(13) | 2.634(10) |
| O(1w)···O(14c)[a] | 2.753(9) |
| O(2w)···O(3d)[a] | 2.672(9) |
| O(2w)···O(4) | 2.760(9) |

[a] Symmetry code: (c) $-x + 1, -y, -z$; (d) $-x, -y + 1, -z$.

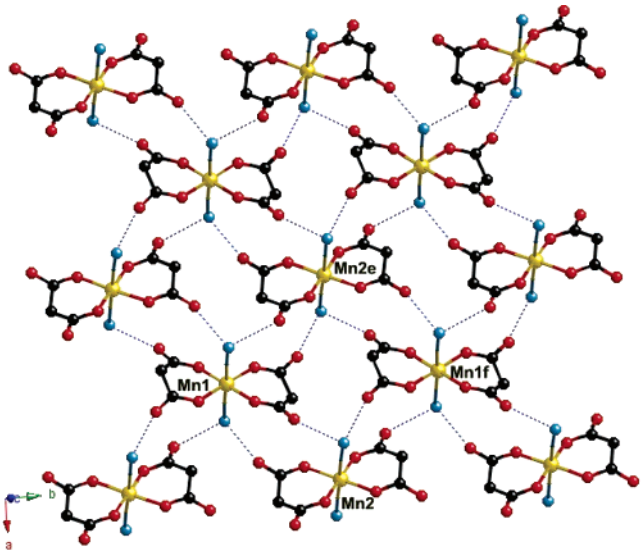


**Figure 2.** Perspective view of the manganese(III) malonato-bridged layer of **2** growing in the *ab* plane. Hydrogens bonds are drawn as blue broken lines.

The $AsPh_4^+$ cations exhibit the expected tetrahedral shape, and its bond distances are in agreement with those observed in previous $AsPh_4^+$-containing compounds.[42] Multiple phenyl embraces involving $AsPh_4^+$ lead to a two-dimensional

(39) Stiefel, E. I.; Brown, G. F. *Inorg. Chem.* **1972**, *2*, 434.

(40) Cremer, D.; Pople, J. A. *J. Am. Chem. Soc.* **1975**, *97*, 1354.

(41) Goedkoop, J. A.; MacGillavry, C. H. *Acta Crystallogr.* **1957**, *10*, 125.

(42) (a) Baldas, J.; Colmanet, S. F.; Mackay, M. F. *J. Chem. Soc., Dalton Trans.* **1988**, 1725. (b) Vicente, R.; Ribas, J.; Alvarez, S.; Seguí, A.; Solans, X.; Verdaguer, M *Inorg. Chem.* **1987**, *26*, 4004. (c) Grenz, R.; Götzfried, F.; Nagel, U.; Beck, W. *Chem. Ber.* **1986**, *119*, 1217.; (d) Muñoz, M. C.; Julve, M.; Lloret, F.; Faus, J.; Andruh, M. *J. Chem. Soc., Dalton Trans.* **1998**, 3125. (e) De Munno, G.; Armentano, D.; Julve, M.; Lloret, F.; Lescouëzec, R.; Faus, J. *Inorg. Chem.* **1999**, *38*, 2234. (f) Marinescu, G.; Andruh, M.; Lescouëzec, R.; Muñoz, M. C.; Cano, J. Cano; Lloret, F.; Julve, M. *New* J. Chem. **2000**, *24*, 527. (g) Lescouëzec, R.; Marinescu, G.; Muñoz, M. C.; Luneau, D.; Andruh, M.; Lloret, F.; Faus, J.; Julve, M.; Mata, J. A.; Llusar, R.; Cano, J. *New. J. Chem.* **2001**, *25*, 1224.

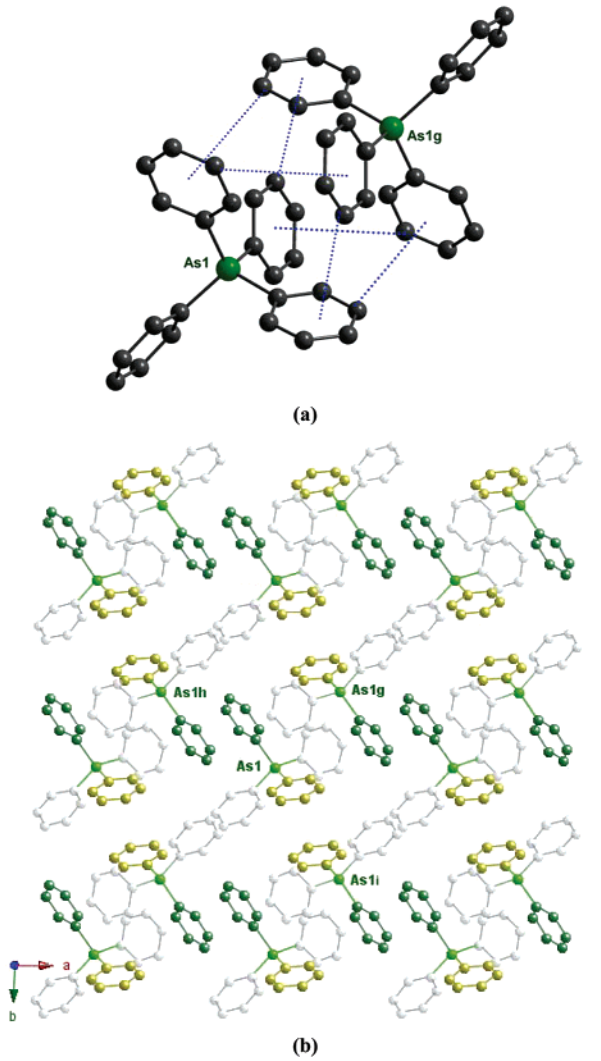


**Figure 3.** (a) Perpective view of the sextuple-phenyl embrace between $AsPh_4^+$ groups. (b) Perspective view of a $AsPh_4^+$ layer of **2** growing in the *ab* plane, showing the multiple phenyl embrace. Double-phenyl embraces (DPE) along the *a* (green rings) and *b* axes (yellow rings) between $AsPh_4^+$ cations are shown.

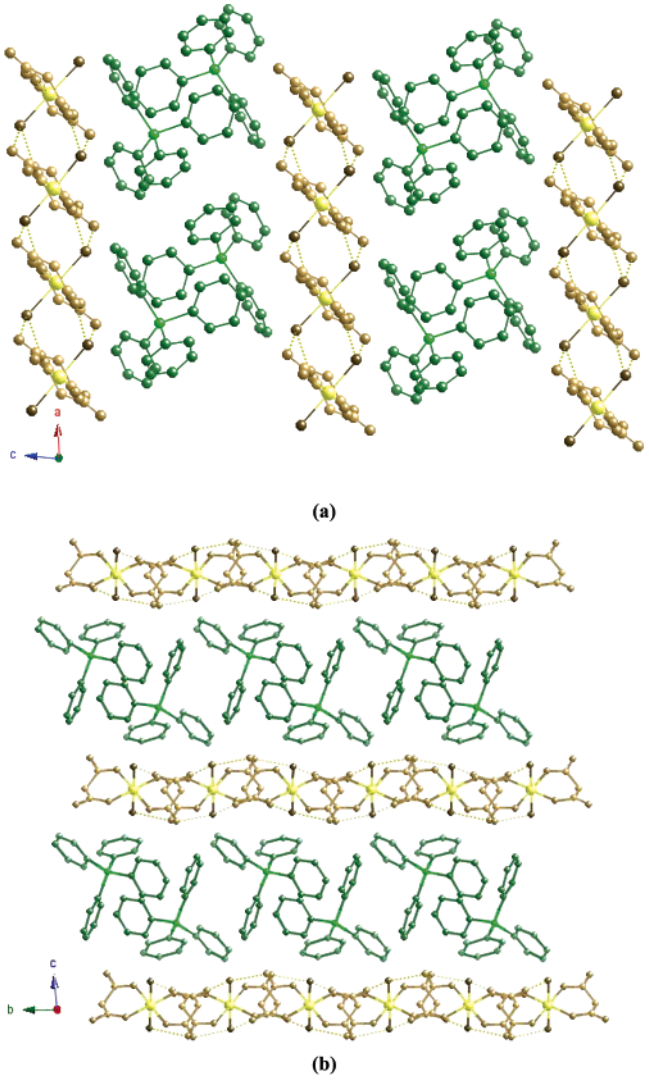


**Figure 4.** (a) Perspective view of the stacking of the manganese(III) malonato-bridged anionic (yellow) and $AsPh_4^+$ cationic (green) layers of **1** along the *a* axis. (b) Perspective view of the stacking of the anionic (yellow) and cationic (green) layers of **1** along the *b* axis. Hydrogen bonds are drawn as yellow broken lines.

cationic network (see Figure 3). Interestingly, alternating sextuple (SPE)- and double-phenyl embraces (DPE)[43] between $AsPh_4^+$ cations occur along the *a* and *b* axis, the arsonium−arsonium distances involved being 6.4369(15) [(SPE):As(1)···As(1g); (g) $-x + 1, -y, -z + 1$], 8.6321(15) [(DPE) along the *a* axis: As(1)···As(1h); (h) $-x, -y, -z + 1$], and 7.5371(15) Å [(DPE) along the *b* axis: As(1)···As(1i); (i) $-x + 1, -y + 1, -z + 1$]. In the case of a DPE where the offset face-to-face interaction occurs between two phenyl rings of two adjacent cations, the interplanar distances are 3.961(13) (along the *a* axis) and 4.95(2) Å (along the *b* axis). Regular alternating anionic and cationic layers occur along the *c* axis, as shown in Figure 4.

We finish this structural discussion by recalling the structure of $K_2[Mn(mal)_2(MeOH)_2][Mn(mal)_2]$[14b] (**3**) and comparing it with that of **2**. The structure of **3** is made up of chains of regular alternating $[Mn(mal)_2(MeOH)_2]^-$ and $[Mn(mal)_2]^-$ units, bridged by anti−syn carboxylate−malonate groups that are connected together by potassium atoms (see Figure 5). Two crystallographically independent manganese(III) atoms are present in **3**, the manganese atoms being located on a crystallographic inversion center. Both metal atoms are six-coordinated, and they exhibit a slightly distorted 4 + 2 elongated octahedron. Four oxygen atoms from two bidentate malonate ions (the bite angle at the metal atom is 91.5(2)°) conform the equatorial plane around Mn(1) (the Mn(1)−O(equatorial) bond distances are 1.901(5) and 1.913(5) Å), the apical positions being occupied by two malonate oxygen atoms (the Mn(1)−O(apical) bond distance being 2.262(5) Å). Mn(2) is bound to four oxygen atoms from two bidentate malonate groups (bite angle = 92.1(2)°) in the equatorial plane (the Mn(2)−O(equatorial) bond distances are 1.901(4) and 1.918(5) Å) and to two oxygen atoms from two methanol molecules (2.203(7) Å for Mn(2)−O(MeOH)) in the axial positions.

The $[Mn(mal)_2(MeOH)_2]^-$ and $[Mn(mal)_2]^-$ units are bridged by *anti*−*syn* carboxylate groups (Figure 5a), which involve an apical oxygen atom at Mn(1) and an equatorial

(43) (a) Dance, I.; Scudder, M. *Chem. Eur. J.* **1996**, *2*, 481. (b) Dance, I.; Scudder, M. *J. Chem. Soc.* Dalton Trans. **1998**, 1341.

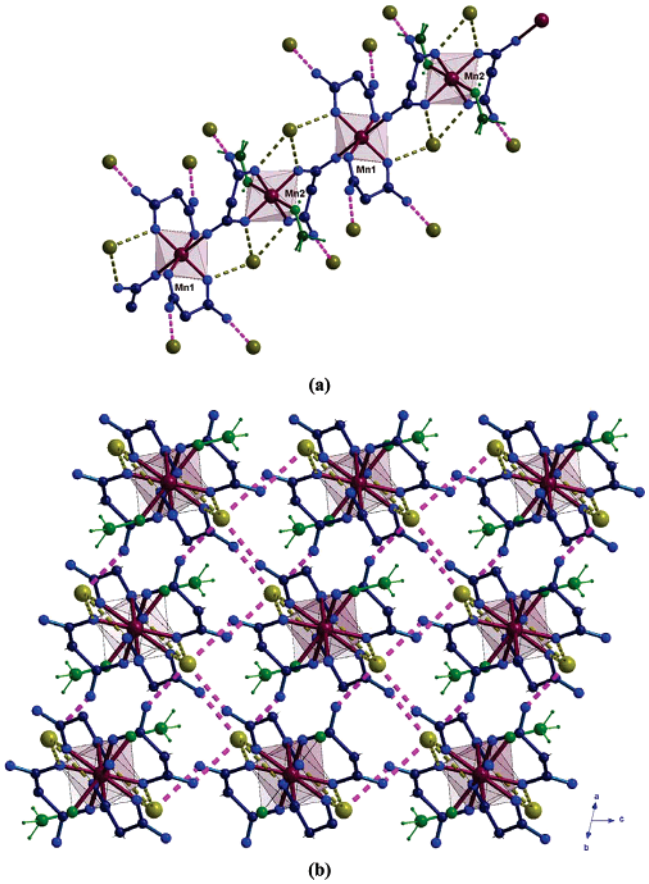


**Figure 5.** (a) Perspective view of a fragment of the alternating carboxylate-(malonate)-bridged manganese(III) chain of **3** growing along the [110] direction. (b) Perspective view of the arrangement of the manganese(III) chains and the potassium cations. Bronze and purple broken lines represent the intra- and interchain O−K−O-bridging units.

one at Mn(2), affording an alternating manganese(III) chain which grows along the [110] direction. These units are further connected through O−K−O bridges (see bronze broken lines in Figure 5) and hydrogen bonds involving the hydroxyl group of the methanol molecule and the malonate oxygen atoms. The intrachain Mn(1)···Mn(2) separation through the carboxylate−malonate group is 5.501 Å, and the dihedral angle between the adjacent mean equatorial planes is 49.4°. The manganese(III) chains are held together by potassium cations. Each chain is connected to nine adjacent ones through O−K−O bridges (see purple broken lines in Figure 5b) leading to a three-dimensional network. The shortest interchain Mn···Mn separations are 6.552 and 8.562 Å for Mn(1)···Mn(2a) and Mn(1)···Mn(2b), respectively ((a) $x + 1, y, z$; (b) $x, y, z + 1$).

In contrast with **2**, where the $[Mn(III)(mal)_2](H_2O)_2]^-$ units are connected by hydrogen bonds involving the water molecules and the uncoordinated malonate-oxygens to create a quasi-square layer of manganese(III) ions, the $[Mn(III)(mal)_2](CH_3OH)_2]^-$ entities in **3** are linked to the $[Mn(III)(mal)_2]^-$ units through *anti*−*syn* carboxylate bridges affording chains. The main difference between **2** and **3** is the character and size of the counterion present in both compounds. In **2**, the hydrophobic and aromatic character of the $AsPh_4^+$ cation are at the origin of the two-dimensional structure with alternating hydrophobic and hydrophilic units.

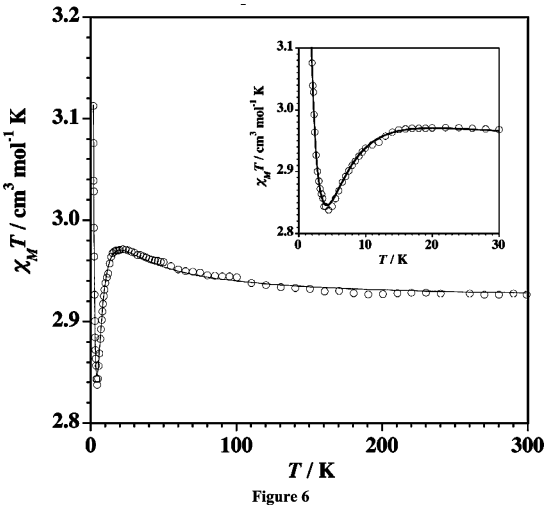


Figure 6

**Figure 6.** Thermal dependence of the $\chi_M T$ product for **1**: (○) experimental data; (—) best-fit curve (see text). (Inset) Low-temperature region in detail.

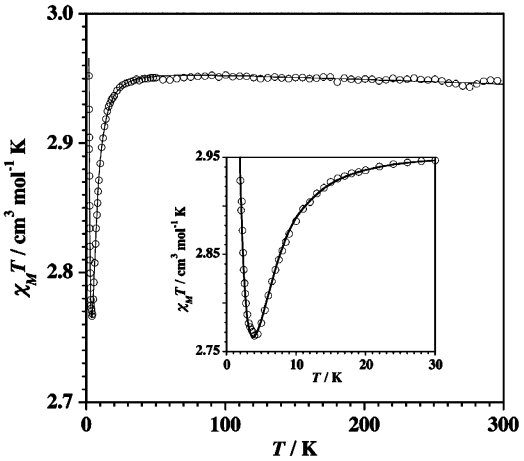


**Figure 7.** Thermal dependence of the $\chi_M T$ product for **2**: (○) experimental data; (—) best-fit curve (see text). (Inset) Low-temperature region in detail.

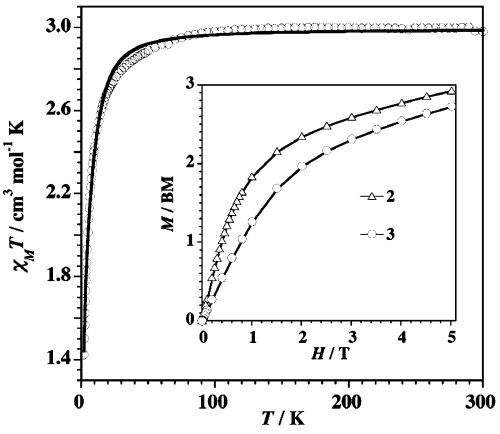


**Figure 8.** Thermal dependence of the $\chi_M T$ product for **3**: (○) experimental data; (—) best-fit curve (see text). (Inset) Magnetization versus $H$ plot at 2.0 K for **3** (○) and **2** (Δ). The solid line is an eye-guide line.

**Magnetic Properties of 1−3.** The magnetic properties of **1**−**3** are shown in Figures 6−8 under the form of $\chi_M T$ versus $T$ plot ($\chi_M$ is the magnetic susceptibility per Mn(III) ion). The values $\chi_M T$ at 300 K are 2.93 (**1**), 2.95 (**2**), and 3.0 $cm^3$ $mol^{-1}$ K (**3**). They are in agreement for the spin-only value of a magnetically isolated high-spin $d^4$ ion ($\chi_M T = 3.0$ $cm^3$ $mol^{-1}$ K with $g = 2.0$). Upon cooling, $\chi_M T$ for **1** smoothly

increases to reach a maximum value of ca. 2.97 $cm^3\ mol^{-1}$ K at 17 K, then it decreases to a minimum of 2.85 $cm^3\ mol^{-1}$ K at 4.5 K, and it increases further to 3.12 $cm^3\ mol^{-1}$ K at 1.9 K. In the case of **2**, the value of $\chi_M T$ remains practically constant from room temperature to 30 K, then it decreases to reach a minimum of ca. 2.76 $cm^3\ mol^{-1}$ K at 4.0 K, and it increases further to 2.95 $cm^3\ mol^{-1}$ K at 1.9 K. Finally, in the case of **3**, a Curie law behavior is observed from room temperature to 90 K followed by a sharp decrease of $\chi_M T$ at lower temperatures to reach 1.4 $cm^3\ mol^{-1}$ K at 1.9 K. The magnetic plots of **1** and **2** are as expected for the coexistence of large single-ion zero-field splitting (ZFS) effects ($D$) and ferromagnetic coupling, whereas in the case of **3**, the significant reduction of $\chi_M T$ at $T < 90$ K is attributed to the simultaneous occurrence of $D$ and antiferromagnetic interactions. An inspection of the $M$ versus $H$ plot at 2.0 K for **2** and **3** (see inset of Figure 8) supports the occurrence of a weak ferromagnetic interaction in **2**, given that its magnetization data are well above those of **3**. No susceptibility maximum is observed in the magnetic plots of **1**−**3** in the temperature range explored. Finally, the lack of *ac* signals for **1**−**3** down to 1.9 K reveals the absence of magnetic ordering in the temperature range explored in this series.

The appropriate Hamiltonian to account for all of these factors is given by eq 1

$$\hat{H} = D\sum_{i=1}^{N}[\hat{S}_{iz}^{\ 2} - 1/3S(S+1)] + E\sum_{i=1}^{N}[\hat{S}_{ix}^{\ 2} - \hat{S}_{iy}^{\ 2}] - J\sum_{i=1}^{N}[\hat{S}_i\hat{S}_{i+1}] + g_{\parallel}\beta\sum_{i=1}^{N}\hat{S}_z H_z + g_{\perp}\beta\sum_{i=1}^{N}(\hat{S}_x H_x + \hat{S}_y H_y) \quad (1)$$

where the two first terms take into account the axial and rhombic ZFS of the single-ion spin state $S = 2$, the third one takes into account states for the magnetic-exchange interaction, and the two last ones correspond to the Zeeman effect. $D$, $E$, $g_{\parallel}$, and $g_{\perp}$ apply for each ion. The application of this Hamiltonian becomes very complicated because of the large number of parameters involved. As the dependence of the magnetic susceptibility on the rhombic splitting parameter ($E$) is negligible, this term was discarded. In addition, we considered that $D$, $g_{\parallel}$, and $g_{\perp}$ are the same for the two manganese sites in **2** and **3** and $g_{\parallel} = g_{\perp}$ (and also in **1**, whose structure is most likely like that of **2**). Under these assumptions, the number of parameters is reduced to a reasonable size, namely $D$, $J$, and $g$.

Taking into account that the size of local interacting spins in **1**−**3** ($S = 2$) is large enough to be considered as a classical spin and that we are dealing with a uniform chain (**3**) and quasi-quadratic layers (**1** and **2**), eqs 2 and 3, which were derived by Fisher[44] and Curély[45] for isotropic Heisenberg systems, can be used to analyze their magnetic properties.

$$\chi_{chain} = \frac{N\beta^2 g^2}{3kT} S(S+1)\frac{1+u}{1-u} \quad (2)$$

$$\chi_{2Dsquare} = \frac{N\beta^2}{3kT} S(S+1)\frac{(g_1^{\ 2} + g_2^{\ 2})W_1 + 2g_1g_2W_2}{2(1-u_1^{\ 2})(1-u_2^{\ 2})} \quad (3)$$

where

$$W_1 = (1+u_1^{\ 2})(1+u_2^{\ 2}) + 4u_1u_2$$

$$W_2 = 2u_1(1+u_2^{\ 2}) + 2u_2(1+u_1^{\ 2})$$

and

$$u_i = \coth\left[\frac{J_i S(S+1)}{kT}\right] - \frac{kT}{J_i S(S+1)}$$

The influence of the ZFS on the powder susceptibility measurements is expressed by eqs 4−6

$$\chi_{\parallel} = \frac{2N\beta^2 g_{\parallel}^{\ 2}}{kT}\frac{\exp(-D/kT) + 4\exp(-4D/kT)}{1 + 2\exp(-D/kT) + 2\exp(-4D/kT)} \quad (4)$$

$$\chi_{\perp} = \frac{2N\beta^2 g_{\perp}^{\ 2}}{3D}\frac{9 - 7\exp(-D/kT) - 2\exp(-4D/kT)}{1 + 2\exp(-D/kT) + 2\exp(-4D/kT)} \quad (5)$$

$$\chi_{ZFS} = \frac{\chi_{\parallel} + 2\chi_{\perp}}{3} \quad (6)$$

Keeping in mind that the magnetic plots in **1**−**3** are dominated by $D$ (the ferro (**1** and **2**)- and antiferromagnetic (**3**) interactions are predicted to be very weak in light of their structures and shape of their magnetic plots), a perturbational approach[11d,46] would be a suitable model to analyze their magnetic data (eqs 7 and 8).

$$\chi_{comp(3)} = \chi_{ZFS}\frac{1+u}{1-u} \quad (7)$$

$$\chi_{comp(1,2)} = \chi_{ZFS}\frac{(g_1^{\ 2} + g_2^{\ 2})W_1 + 2g_1g_2W_2}{2(1-u_1^{\ 2})(1-u_2^{\ 2})} \quad (8)$$

with

$$g_1 = g_2$$

and

$$u_1 = u_2$$

Thus, the magnetic behavior of **1**−**3**, which is dictated by the dominant $D$ factor, is slightly perturbed by the weak magnetic interactions observed in the very-low-temperature region. Best-fit parameters through eqs 8 (**1** and **2**) and 7 (**3**) are: $D = -3.91(2)\ cm^{-1}$, $J = +0.081(1)\ cm^{-1}$, and $g = 1.98(1)$ for **1**, $D = -3.96(2)\ cm^{-1}$, $J = +0.072(1)\ cm^{-1}$, and $g = 1.99(1)$ for **2** and $D = -3.95(2)\ cm^{-1}$, $J = -0.19(1)\ cm^{-1}$, and $g = 1.99(1)$ for **3**. As seen in Figures 6−8, a satisfactory match is obtained between the magnetic data and the theoretical curve in the whole temperature range explored. We have used a negative $D$ value in the fits because it is more usual, but a similar fit is obtained when considering a positive value for $D$.

**Analysis of the Exchange Pathways in 2 and 3.** To substantiate the magnetic interactions between manganese-

(44) Fisher, M. E. *Am. J. Phys.* **1964**, *32*, 343.
(45) (a) Curély, J. *Europhys. Lett.* **1995**, *32*, 529. (b) Curély, J. *Physica B* **1998**, *245*, 263.
(46) Lloret, F.; Ruiz, R.; Julve, M.; Faus, J.; Journaux, Y.; Castro, I.; Verdaguer, M. *Chem. Mater.* **1992**, *4*, 1150.

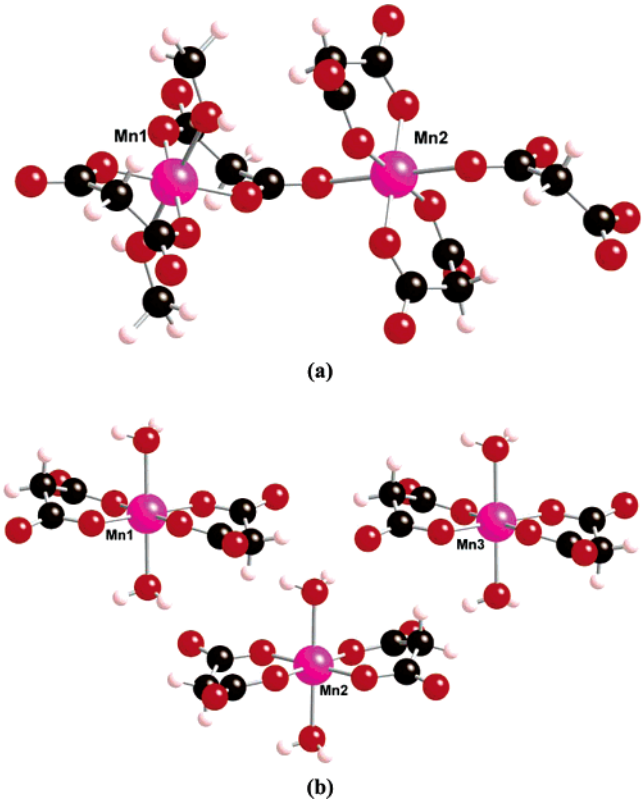


**Figure 9.** Structural models used in the DFT calculations concerning **3** (a) and **2** (b). Bond lengths and angles of the models are those of the corresponding crystal structures.

(III) ions in **2** and **3** and to get an orbital picture of the exchange pathways involved in them, we have performed density functional theory-type (DFT) calculations on two model fragments whose structural parameters were taken from the respective crystal structures: a dinuclear unit of the chain structure of **3** (Figure 9a) and a trinuclear manganese(III) entity corresponding to the two edges of the quasi-square units of the anionic layers of **2** (Figure 9b).

Let us start the analysis with **3** for the sake of simplicity. This compound can be considered as a one-dimensional system where two crystallographically independent manganese(III) ions are connected in a regular way by a carboxylate group of a malonate ligand that exhibits the *anti*−*syn* bridging mode. A nonet A (2,2) and a broken-symmetry singlet B (2,−2) spin configurations were calculated (A and B being defined as ($M_{S\ Mn1}$, $M_{S\ Mn2}$)). From the energies of these configurations and eq 9

$$E_B - E_A = -10J \qquad (9)$$

we have evaluated the exchange coupling constant between the manganese(III) ions in **3**, which is $J = -4.7$ cm$^{-1}$. This value has the same sign and it is not far from that obtained for **3** by fit ($J = -0.19$ cm$^{-1}$) and also for the family of the chain compounds of formula $(cat)_2[Mn^{III}(sal)_2(CH_3OH)_2]$-$Mn^{III}(sal)_2]$ with sal = salicylate and cat = $Na^+$ ($J = -0.46$ cm$^{-1}$), $K^+$ ($J = -0.46$ cm$^{-1}$), and $NH_4^+$ ($J = -1.40$ cm$^{-1}$),[14b] where the same type of carboxylate−malonate bridge occurs. An inspection of the magnetic orbitals involved accounts for the antiferromagnetic nature of the magnetic coupling. In

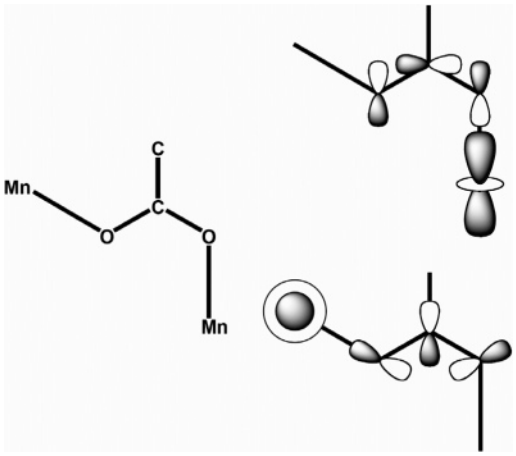


**Figure 10.** Schematic drawing showing the orientation of the $d_{z^2}$-type magnetic orbitals in the dinuclear fragment of **3** (model Figure 5a).

fact, the manganese(III) ions in **3** (also in **2**) exhibits elongated octahedral environments with an idealized $D_{4h}$ symmetry. Consequently, if one takes the elongation axis as the *z* direction, one unpaired electron is placed in the $d_{z^2}$ orbital and the $d_{x^2-y^2}$ orbital is non magnetic, given that this last orbital has the highest energy. The relative orientation of the two $d_{z^2}$ magnetic orbitals is represented in Figure 10. Although an *anti*−*syn* coordination topology occurs in **3** with the two metal ions and the carboxylate group being practically coplanar, the strict orthogonality is avoided because of the values of the Mn−O−C angles (127.3(5) and 137.8(5)°).[14a] One can see that the equatorial ring $d_{z^2}$ electron density in a manganese atom and the axial $d_{z^2}$ in the other manganese center are involved in the exchange pathway; thus, a small overlap between the two magnetic orbitals through the carboxylate−malonate bridge is predicted, and a weak antiferromagnetic interaction is expected, as observed. Indeed, the small magnitude of the magnetic interaction is also related to the weak spin delocalization observed in the atomic spin densities (3.98 electron units for the manganese(III) ion).

The hydrogen bonds between the mononuclear $[Mn^{III}(mal)_2(H_2O)_2]^-$ units in **2** have to be responsible for the ferromagnetic coupling observed for this compound. Recently, Desplanches et al. have shown that hydrogen bonds can mediate weak magnetic interactions in metal complexes.[47] As described in the structural part, the $[Mn^{III}(mal)_2(H_2O)_2]^-$ units in **2** are linked by hydrogen bonds to form an anionic quasi-quadratic layer of manganese(III) ions (Figure 2) with two intralayer magnetic interactions noted $J_1$ (between Mn(1) and Mn(2)) and $J_2$ (between Mn(1) and Mn(2e)). These layers are well separated from each other by the bulky tetraphenylarsonium cations (Figure 4). The only intralayer exchange pathway occurring in **2** involves the axially coordinated water molecule of one manganese unit and a carboxylate−malonate from the neighboring unit. Two of these pathways connect each pair of manganese(III) ions. Small structural differences in them lead to an alternating character of the network. Thus, in the model used for **2**, three

(47) Desplanches, E.; Ruiz, E.; Rodríguez-Fortea, A.; Alvarez, S. *J. Am. Chem. Soc.* **2002**, *124*, 5197.

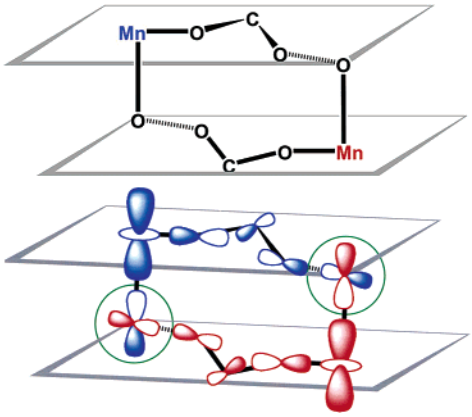


**Figure 11.** (Top) Schematic drawing of a $Mn(OCO\cdots Ow)_2Mn$ couple in **2**. (Bottom) Orbital picture of the exchange pathway in **2**.

metal ions and two exchange coupling constants have been considered (Figure 9b). Using eqs 10 and 11

$$E_D - E_C = -10J_1 \quad (10)$$

$$E_F - E_C = -10J_2 \quad (11)$$

applied to the energy obtained for the configurations C (2,2,2), D (−2,2,2), and F (2,2,−2) (C, D, and F being defined as ($M_{S\ Mn1}$, $M_{S\ Mn2}$, $M_{S\ Mn3}$, respectively)), we have obtained the values +0.04 and +0.02 $cm^{-1}$ for $J_1$ and $J_2$, respectively. Thus, weak ferromagnetic interactions between the metal ions are obtained by DFT calculations whose values are close to the mean value obtained by fit. A close inspection of the dinuclear fragment $Mn-(OCO\cdots O_w)_2-Mn$ of **2**, depicted on the top of Figure 11, shows that the two $Mn-OCO\cdots O_w$ units are in parallel planes, and the axial $Mn-O_w$ bonds are quasi-perpendicular to these planes. The corresponding orbital picture is shown in the bottom of Figure 11. One can see there that the spin density in the ring of the $d_{z^2}$ orbital leads to a delocalization via a $\sigma$-exchange pathway of carboxylate (blue), whereas the axial spin density in the same orbital involves a delocalization via a $\pi$-exchange pathway (red). This situation corresponds to a case of orthogonality between the interacting magnetic orbitals, and consequently, a ferromagnetic coupling is predicted, as observed.

## Conclusions

A new malonate-containing manganse(III) building block of formula $AsPh_4[Mn(mal)_2(H_2O)_2]$ (2) has been prepared and magneto−structurally characterized. Hydrogen bonds appear as effective mediators of weak but significant ferromagnetic interactions between the manganese(III) ions, which were substantiated by DFT-type calculations. A weak intrachain antiferromagnetic coupling through the carboxylate−malonate bridge occurs in the related compound of formula $K_2[Mn(mal)_2(MeOH)_2][Mn(mal)_2]$ (**3**), whose structure was the subject of a previous report. The hydrophobic and hydrophilic characters of the $AsPh_4^+$ and $K^+$ cations seem to be at the origin of the layered and one-dimensional structures of **2** and **3**, respectively.

**Acknowledgment.** This work was supported by the Ministerio Español de Educación y Ciencia, (Projects CTQ2004-03633 and MAT2004-03112). F.S.D. acknowledges the Gobierno Autónomo de Canarias for a predoctoral fellowship.

**Supporting Information Available:** Table S1. Weak hydrogen bonds (Å) involving C-aromatic and oxygen atoms for **1**. This material is available free of charge via the Internet at http://pubs.acs.org.

IC0508526